

LEVEL III

12

AD

A100235

TECHNICAL REPORT
TR 75-55-CEMEL

S

AD A100235

**PERSPIRATION POISONING OF PROTECTIVE CLOTHING
MATERIALS - PART II -
MATHEMATICAL MODEL FOR A COMPLEX ADSORPTION BED**

DTIC
ELECTE
JUN 16 1981
S **D**
E

Approved for public release;
distribution unlimited.

June 1974

UNITED STATES ARMY
NATICK RESEARCH and DEVELOPMENT COMMAND
NATICK, MASSACHUSETTS 01760



Clothing, Equipment and Materials Engineering Laboratory

CEMEL 166

81 6 15 158

DTIC FILE COPY

Approved for public release; distribution unlimited.

Citation of trade names in this report does not constitute an official indorsement or approval of the use of such items.

Destroy this report when no longer needed. Do not return it to the originator.

REPORT DOCUMENTATION PAGE		READ INSTRUCTIONS BEFORE COMPLETING FORM
1. REPORT NUMBER TR-75-55-CEMEL ✓	2. GOVT ACCESSION NO. AD-A100 235	3. RECIPIENT'S CATALOG NUMBER
4. TITLE (and Subtitle) PERSPIRATION POISONING OF PROTECTIVE CLOTHING MATERIALS, PART II, MATHEMATICAL MODEL FOR A COMPLEX ADSORPTION BED	5. TYPE OF REPORT & PERIOD COVERED Final Technical Report 1 July 1972 - 30 June 1974	6. PERFORMING ORG. REPORT NUMBER CEMEL 166 ✓
7. AUTHOR(s) J. K. Ferrell, M. R. Branscome and R. W. Rousseau	8. CONTRACT OR GRANT NUMBER(s) DAAG17-72-G-0004 ✓	
9. PERFORMING ORGANIZATION NAME AND ADDRESS Department of Chemical Engineering North Carolina State University Raleigh, North Carolina 27607	10. PROGRAM ELEMENT, PROJECT, TASK AREA & WORK UNIT NUMBERS 62105A TT162105AH8402-107	
11. CONTROLLING OFFICE NAME AND ADDRESS U.S. Army Natick R&D Command ATTN: DRXNM-VMP Natick, Massachusetts 01760	12. REPORT DATE June 1974	13. NUMBER OF PAGES 53
14. MONITORING AGENCY NAME & ADDRESS (if different from Controlling Office)	15. SECURITY CLASS. (of this report) Unclassified	15a. DECLASSIFICATION/DOWNGRADING SCHEDULE N/A
16. DISTRIBUTION STATEMENT (of this Report) Approved for public release; distribution unlimited.		
17. DISTRIBUTION STATEMENT (of the abstract entered in Block 20, if different from Report)		
18. SUPPLEMENTARY NOTES		
19. KEY WORDS (Continue on reverse side if necessary and identify by block number) CARBON ADSORPTIVITY ADSORPTION ISOTHERMS ADSORPTION BREAKTHROUGH TIME POISONING ACTIVATED CARBON SWEAT POISONING FOAM		
20. ABSTRACT (Continue on reverse side if necessary and identify by block number) A mathematical model is developed using the method of moments for the adsorption of carbon tetrachloride vapor by carbon impregnated foam material. This material was developed by the U. S. Army Natick R&D Command for use as a protective overgarment to adsorb toxic agents. Problems associated with the modeling of this system include the following uncertainties: (1) amount of carbon in a sample, (2) carbon particle size and distribution, and (3)		

408153

43

UNCLASSIFIED

SECURITY CLASSIFICATION OF THIS PAGE(When Data Entered)

#20 Abstract (continued)

characterization of flow through a foam matrix embedded with carbon. A method of grouping constants with the rate parameters was devised to give a coefficient representative of the rate parameter contained within the grouping. It was found that the adsorption models obtained by assuming the rate determining mechanism of adsorption to be either diffusion from the bulk gas to the particle, pore diffusion, or surface adsorption were not significantly different. A model based on an overall mass transfer coefficient was developed, and when this coefficient was evaluated from the first moment equation, the overall coefficient model fit the data well. This procedure offers an alternative approach to modeling an adsorption process in which the true controlling mechanisms of mass transfer are not known.

UNCLASSIFIED

SECURITY CLASSIFICATION OF THIS PAGE(When Data Entered)

TABLE OF CONTENTS

	Page
LIST OF FIGURES -----	4
LIST OF TABLES -----	5
INTRODUCTION -----	6
EXPERIMENTAL -----	10
DISCUSSION -----	13
RESULTS -----	21
CONCLUSIONS -----	25
REFERENCES -----	26
LIST OF SYMBOLS -----	27
TABLES -----	29
FIGURES -----	37
APPENDIX A Derivation of Zeroth and First Moment Equations -----	47
APPENDIX B Explanation of Numerical Work -----	53

Accession For	
NTIS GRA&I	<input checked="" type="checkbox"/>
DTIC TAB	<input type="checkbox"/>
Unannounced	<input type="checkbox"/>
Justification	<input type="checkbox"/>
By	
Date	
Dist	
A	

LIST OF FIGURES

	Page
1. Schematic of Vapor Test Apparatus	38
2. Model Prediction and Experimental Data for One Layer Run	39
3. Model Prediction and Experimental Data for Three Layer Run	40
4. Model and Experimental Data for Different Conditions	41
5. Model and Experimental Data for Different Conditions	42
6. Model and Experimental Data for Different Conditions	43
7. Effect of Changing K_A 10% as Predicted by Mathematical Model	44
8. Effect of Changing UA 25 % as Predicted by Mathematical Model	45
9. Correlation of UA from Statistical Analysis	46

LIST OF TABLES

	Page
1. Components of Experimental Apparatus (Figure 1).	30
2. Comparison of Models.	31
3. Comparison of Model Results - Varying UA.	33
4. Comparison of Model Results - Varying K_A .	34
5. Comparison of Model Results - Varying K_A and UA.	35
6. Model Prediction of Breakthrough Time for Bolt 3 Foam Material.	36

PERSPIRATION POISONING OF PROTECTIVE CLOTHING MATERIALS

PART II

MATHEMATICAL MODEL FOR A COMPLEX ADSORPTION BED

INTRODUCTION

The mathematical modeling of adsorption processes is well documented and the literature on the subject is extensive. One of the most complete and useful approaches is that proposed by Schneider and Smith¹ for a bed of particles in which adsorption takes place as a three-step mechanism: (1) diffusion from the bulk gas phase to the external surface of the particle, (2) diffusion into the particle, and (3) adsorption on the particle's surface. Masamune and Smith² have presented models that describe the above mechanisms as controlling resistances, both singly and in pairs, and offer an alternate approach to modeling an adsorption process. If an adsorption process can be characterized by a single controlling resistance, the mathematical work and subsequent model are greatly simplified. This in turn gives the investigator a better understanding of the ways in which the physical properties of his adsorption system affect the adsorption process. The utility of such models for well-defined systems has been demonstrated by the excellent agreement of experimental and theoretical transmission curves of C/C_0 vs. time obtained by Schneider and Smith¹ and Masamune and Smith.² However, problems arise in this procedure when the adsorption system is complex,

¹Schneider, P., and J. M. Smith, AICHE J., 14, 762 (1968).

²Masamune, S., and J. M. Smith, AICHE J., 11, 34 (1965).

not well-defined, and of questionable homogeneity. The work performed during this study was on such a system in which the adsorbent was activated carbon impregnated in foam material with a nylon backing. Inherent uncertainties for this system included the amount of carbon in a foam sample, carbon particle size, non-homogeneity of foam material samples, and the characterization of flow through a foam matrix embedded with charcoal.

The adsorbent material was developed by the U. S. Army Natick R&D Command for use as a protective overgarment to adsorb chemical agents, especially poisonous gases. The material was found very effective for short periods of time, but due to its thermal insulating properties its adsorptive capacity for toxic gases was reduced because of "poisoning" human perspiration. The long-time objective of the grant that funded this research is to remedy this "poisoning" problem; therefore, the modeling work considers the different types of conditions described in the experimental procedure.

The material consisted of a layer of polyurethane foam bonded to a nylon tricot and impregnated with activated carbon held on the material with a polymer latex binder. Thickness of the material was approximately 0.18 cm. Samples of this carbon impregnated foam were received as bolts of material which were found to have wide variations in adsorptive capacity. Work done during this study was on the second and third bolts received from Natick and will be referred to as bolt 2 and bolt 3, respectively. A detailed description of the material is given in Part I of this report.

The initial model work was directed toward developing the three parameter model of Schneider and Smith¹ and applying it to the adsorption of

¹op. cit.

carbon tetrachloride vapor by charcoal impregnated foam. It was decided to use the method of moments to evaluate the three rate parameters from the experimental data. This procedure required three independent moment equations and consistent data with a minimum of error magnification for higher moments. The zeroth moment equation gave an expression for determining K_A , the equilibrium adsorption constant, and the first, second, and third moment equations gave independent expressions for the three rate parameters. The solution of these equations yielded negative and imaginary values for two of the rate parameters and revealed the inadequacy of the data for use in evaluating more than the first moment numerically. This made necessary a simplified approach of assuming a single resistance rate controlling and evaluating this resistance from the first moment equation. Diffusion into the particle was assumed to be the rate determining mechanism and the model equations were solved. The model worked well in predicting breakthrough curves, but it was found that the models obtained by assuming either external diffusion or surface adsorption rate controlling also fit the data well. Differentiation between models was further complicated by an inability to change the adsorbent's physical properties and by a limited range of temperature and flow in the adsorption apparatus.

Subsequent mathematical work showed that when the rate parameter was evaluated from the first moment, the external diffusion and surface adsorption models were exactly the same, and that the model assuming pore diffusion controlling, while not mathematically identical, was not significantly different from the other two cases. It was then proposed that the first moment equation for the three parameter model be expressed as an overall

coefficient, UA:

$$\frac{W_t}{Q} \left(\frac{M_1}{M_0} - \frac{1}{2} \right) = \left[\frac{1}{k_f A} + \frac{1}{5D_c A/R} + \frac{1}{k_{ads} \delta} \right] = \frac{1}{UA}$$

This overall coefficient would reflect the influence of the three different resistances and would make possible the use of a model with only one rate parameter when the controlling mechanisms of mass transfer were not known. An overall coefficient model was developed and when the rate parameter was evaluated from the first moment, this model was shown to be the same as the model of external diffusion rate controlling and the same as the model of surface adsorption rate controlling. It was also found that the overall coefficient model produced results that were not significantly different from those produced by the pore diffusion controlling model. This procedure offered an alternative approach in modeling an adsorption process in which the adsorbent properties and adsorption conditions could not be varied effectively to determine the true controlling mechanisms of mass transfer.

EXPERIMENTAL

A schematic diagram of the apparatus for the study of the dynamics of carbon tetrachloride vapor adsorption by charcoal impregnated foam material is shown in Figure 1 with a list of components in Table 1. This apparatus consisted of a flow system of stainless steel tubing with an adsorption chamber enclosed in a plexiglass box for constant temperature control. A pure nitrogen stream from the nitrogen supply cylinder was split at the inlet and sent through lines (1) and (2). Nitrogen in line (2) flowed through the carbon tetrachloride bubbler (4) immersed in an ice-bath to saturate the nitrogen stream with carbon tetrachloride vapor at 0°C. The pure nitrogen stream in line (1) flowed through an orifice (5) with a hook-gage manometer (6) and rotameter in series and was mixed with the nitrogen-carbon tetrachloride stream for dilution to the desired concentration. The flow control of the pure nitrogen stream in line (1) was critical because of the high dilution factor. This flow rate was set roughly by the rotameter (8) and then adjusted by measuring the pressure drop across the orifice to one ten-thousandth of an inch of water with the hook-gage manometer.

The diluted nitrogen-carbon tetrachloride mixture was sent into the constant temperature box (25) through a temperature equilibrating coil (14) and into a manifold (17). A vapor stream was drawn from the manifold (at 18) and sent through the sample holder (19) at a flow rate set by rotameter (22). This sample holder consisted of two stainless steel cups between which the foam material was sandwiched, tightened with a clamp, and sealed with wax. The top cup contained a perforated metal sheet to assure uniform gas flow through the sample. The vapor stream leaving the sample holder

was sent through a gas collection coil on the chromatograph and the remainder of the vapor mixture entering the manifold was vented through an exhaust hood (23).

Analysis of the carbon tetrachloride concentration in the stream exiting the sample cup was made by a Perkin-Elmer gas chromatograph using a column of silicone oil D.C. #200 with a thermal conductivity detector. A Moseley strip chart recorder monitored the chromatograph output. Reference peaks for the initial concentration were obtained at the beginning and end of each adsorption run by taking a sample stream from the manifold at (26) and sending it through the chromatograph. Injections were made using the gas sampling valve of the chromatograph at three minute intervals, and from the recorded output (chromatographic curves), transmission curves of $C(t)/C_0$ vs. time were generated.

A method of conditioning the foam samples was devised to improve consistency from sample to sample. The foam material was cut into five inch circles, soaked in distilled water for twenty-four hours, wrung out between rubber rollers, and then allowed to equilibrate in a room maintained at 70°F (21°C) and 65% relative humidity. Treatment with other solutions (e.g., sweat, lactic acid) was accomplished by following the water conditioning with treatment with the proper solution and again allowing the sample to equilibrate at 70°F (21°C) and 65% relative humidity. Thus, valid comparisons could then be made between different treatments and also among conditioned samples for different run conditions.

The adsorption bed was composed of either single or multiple layers of the carbon impregnated foam material: for this study beds of one and three layers were considered. In this manner the effects of different bed depths could be studied.

Carbon tetrachloride was suggested as the adsorbable vapor since correlations exist between carbon tetrachloride and the toxic gases in which the Army was interested.

DISCUSSION

One of the most useful and complete approaches to modeling an adsorption process is that of Schneider and Smith¹ who proposed that the adsorption of a gas flowing through a bed of spherical particles could be modeled as a three step mechanism: diffusion from the bulk gas to the external surface of the particle, pore diffusion into the particle, and adsorption on the particles surface. For the present study the adsorption bed was composed of carbon particles, assumed to be spherical, embedded in an inert matrix of urethane foam. Since very thin beds were used, the effect of axial dispersion was neglected and plug flow was assumed. The presence of inerts in the adsorption bed necessitated defining two void fractions, α and ϵ , where α represents void volume/total volume that must be used in determining the volume in which convection and accumulation take place in the gas phase, and where $1 - \epsilon$ represents carbon volume/total volume which must be used in expressing the rate of removal in terms of the volume of carbon particles. With these modifications a mass balance of the adsorbable component in the gas phase yields:

$$-v \frac{\partial C}{\partial z} - \frac{\partial C}{\partial t} - \frac{3D_c}{R} \frac{1-\epsilon}{\alpha} \left(\frac{\partial C_i}{\partial r} \right)_{r=R} = 0 \quad (1)$$

and a mass balance of this component in the particle:

$$\frac{D_c}{\beta} \left(\frac{\partial^2 C_i}{\partial r^2} + \frac{2}{r} \frac{\partial C_i}{\partial r} \right) - \frac{\partial C_i}{\partial t} - \frac{\rho_p}{\beta} \frac{\partial C_{ads}}{\partial t} = 0 \quad (2)$$

The rate of adsorption (assumed to be linear) is:

$$\frac{\partial C_{ads}}{\partial t} = k_{ads} (C_i - C_{ads}/K_A') \quad (3)$$

with the various boundary conditions listed below:

external diffusion boundary condition:

$$D_c \left(\frac{\partial C_i}{\partial r} \right)_{r=R} = k_f (C - C_i) \quad (4)$$

internal diffusion boundary condition:

$$\frac{\partial C_i}{\partial r} = 0 \text{ at } r = 0 \text{ for } t > 0 \quad (5)$$

initial conditions:

$$C = 0 \text{ at } z > 0 \text{ for } t = 0 \quad (6)$$

$$C_i = 0 \text{ at } r > 0 \text{ for } t = 0 \quad (7)$$

$$C = C_0 \text{ at } z = 0 \text{ for } t > 0 \quad (8)$$

Equations 1 through 8 have been solved by Rosen³ using Laplace transforms and the inversion integral to give an expression for $C(t)$, the gas concentration exiting the bed, in the form of an infinite integral. To use Rosen's expression for $C(t)$, it is necessary to know the values of the three rate parameters, k_f , k_{ads} , and D_c , for the adsorption system of this study. An empirical approach to evaluating these parameters was ruled out due to uncertainties in the adsorbent's properties and shortcomings in the adsorption apparatus. These problems include (1) an inability to change the adsorbent's physical properties, such as particle size and distribution, (2) an uncertainty as to the characterization of flow through a foam matrix embedded with carbon, and (3) a limited range of flow rate and temperature in the adsorption apparatus.

The method of moments offered an alternative approach in that the three rate parameters could be determined analytically for each adsorption run by

³Rosen, J. B., J. Chem. Phys., 20, 387 (1952).

evaluating the first, second and third moments numerically and using the corresponding moment equations to solve directly for k_f , k_{ads} , and D_c . Moment equations were derived for a step input using Aris' theorem⁴ and were found to be:

$$M_0 = \frac{z}{V} \frac{1-\epsilon}{\alpha} \rho_p K_A' = \frac{W_t}{Q} K_A ; \beta \ll \rho_p K_A' \quad (9)$$

$$\left(\frac{M_1}{M_0} - \frac{1}{2}\right) \frac{W_t}{Q} = \frac{1}{k_f A} + \frac{1}{5D_c A/R} + \frac{1}{k_{ads} \delta} \quad (10)$$

$$\left(\frac{M_2}{M_0} - \frac{2M_1}{M_0} + 2/3\right) \frac{W_t^2}{Q^2} = \frac{2}{(k_f A)^2} + \frac{4}{35(D_c A/R)^2} + \frac{2}{(k_{ads} \delta)^2} \quad (11)$$

$$+ \frac{4}{5(D_c A/R)(k_f A)} + \frac{4}{(k_f A)(k_{ads} \delta)} + \frac{4}{5(D_c A/R)(k_{ads} \delta)}$$

$$\left(\frac{M_3}{M_0} - \frac{3M_2}{M_0} - \frac{3M_1^2}{M_0} + \frac{6M_1}{M_0} + \frac{1}{2}\right) \frac{W_t^3}{Q^3} = \frac{6}{(k_f A)^3} + \frac{18}{175(D_c A/R)^3} \quad (12)$$

$$+ \frac{6}{(k_{ads} \delta)^3} + \frac{144}{5(k_f A)^2(D_c A/R)} + \left(\frac{8}{315} + \frac{2}{225}\right) \left(\frac{27}{(k_f A)(D_c A/R)^2}\right)$$

$$+ \frac{18}{(k_f A)^2(k_{ads} \delta)} + \frac{36}{35(D_c A/R)^2(k_{ads} \delta)} + \frac{18}{(k_f A)(k_{ads} \delta)^2}$$

$$+ \frac{6}{5(D_c A/R)(k_{ads} \delta)^2} + \frac{24}{5(D_c A/R)(k_f A)(k_{ads} \delta)}$$

For this system in which constants such as ρ_p , α , ϵ , and R are not known and are very difficult to measure accurately, constants were grouped together

⁴Aris, R., Proc. Roy. Soc. (London), A245, 268 (1958).

and lumped with the rate parameter to give a coefficient that would be representative of the rate parameter contained within the grouping. An additional advantage in this procedure is the conversion from a weight basis of carbon particles (which is not known) to a weight basis of foam material by assuming that δ , grams carbon/gram foam, is constant for any given bolt of carbon impregnated foam material. The following substitutions were made:

If ρ_m = grams foam material/cm³ total volume

$1 - \epsilon$ = cm³ carbon/cm³ total volume

α = cm³ void/cm³ total volume

A_f = bed cross section, cm²

z = bed depth, cm

δ = g carbon/g foam

K_A' = equilibrium adsorption constant, cm³ adsorbed/g carbon

Then the weight of the sample bed, W_t , is:

$$W_t = A_f z \rho_m \quad (13)$$

and the volumetric flow rate through the sample, Q , is:

$$Q = A_f V \alpha \quad (14)$$

$$\text{So that } \frac{W_t}{Q} = \frac{z}{V} \frac{\rho_m}{\alpha} \quad (15)$$

A new equilibrium constant K_A , cm³ adsorbed/gram foam, can be defined on a weight basis of foam material as:

$$K_A = \delta K_A' \quad (16)$$

The apparent foam density is shown to be:

$$\rho_m = (1 - \epsilon) \frac{\text{cm}^3 \text{ carbon}}{\text{cm}^3 \text{ total volume}} \cdot \frac{1 \text{ g foam}}{\delta \text{ g carbon}} \cdot \rho_p \frac{\text{g carbon}}{\text{cm}^3 \text{ carbon}} \quad (17)$$

$$= \frac{1 - \epsilon}{\delta} \rho_p \frac{\text{g foam}}{\text{cm}^3 \text{ total volume}}$$

Substituting (15), (16), and (17) into the zeroth moment equation:

$$M_0 = \frac{Z}{V} \frac{1 - \epsilon}{\alpha} \rho_p K_A' = \frac{W_t}{Q} K_A \quad (18)$$

The quantity A, used in the lumped parameters of the first, second, and third moment equations, is defined as surface area of carbon particles/unit weight of foam material and is shown to be:

$$A = \frac{4\pi R^2 \text{ cm}^2 \text{ surface area}}{4/3 \pi R^3 \text{ cm}^3 \text{ carbon}} \cdot \frac{1 \text{ cm}^3 \text{ carbon}}{\rho_p \text{ g carbon}} \cdot \delta \frac{\text{g carbon}}{\text{g foam}} = \frac{3\delta}{\rho_p R} \quad (19)$$

The substitution of (18) and (19) into the higher moment equations gave the results listed as equations (10), (11), and (12).

Equations for the first, second, and third moments allowed the three rate parameters to be calculated directly from a single adsorption run; however, problems arose because of the generation of imaginary or negative values for $k_f A$ and k_{ads} . This was probably due to inaccuracies in data since the calculation of the second and higher moments necessitates very accurate experimental data. Serious troubles arise from the uncertainty of the exact position of the tails of the transmission curve where a minor change in concentration is enlarged by the second (or higher) power of time. This problem led to the development of a model in which one of the three resistances is considered to be rate determining and can be found from the first moment equation. Masamune and Smith² have obtained solutions for the

three cases where each resistance is considered controlling and these are listed in Table 2.

The k_f and k_{ads} models shown in Table 2 are the same, and when the first moment equation is used to evaluate the controlling resistance as either $k_f A$, k_{ads} , or $D_c A/R$, all three models give approximately the same results. The differentiation between models was further complicated by an inability to change the adsorbent's physical properties (such as particle size and distribution), a limited range of inlet concentration, flow and temperature in the adsorption apparatus, and as previously mentioned, C/C_0 transmission curves that are inadequate for complete moments analysis.

An alternative way of viewing this adsorption process is that the resistances to mass transfer from the bulk gas to the particle's surface may be represented by one overall mass transfer coefficient. The form of the first moment equation for the three parameter model suggests that an overall coefficient, UA , might be written as:

$$\frac{1}{UA} = w_t \left(\frac{M_1}{M_0} - \frac{1}{2} \right) = \frac{1}{k_f A} + \frac{1}{5D_c A/R} + \frac{1}{k_{ads} \delta}$$

The three resistances to adsorption are not in series since pore diffusion contributes a variable resistance that is a function of the spherical coordinate, r , and may occur in parallel with surface adsorption. However, one may picture the pore diffusion resistance term, $1/5D_c A/R$, as an average resistance or the pore diffusion resistance at the effective path length that all molecules must travel before being adsorbed on the surface. Then the definition of an overall coefficient provides a means of accounting for the effects of the three resistances as an average or overall resistance. This overall coefficient when evaluated from the first moment would then

reflect the influences of each of the three resistances and would simplify the modeling in that higher moments equations would be unnecessary in evaluating UA. The development of an overall coefficient model is outlined below:

$$\frac{C_{ads}}{\partial t} = \frac{UA}{\delta K_A'} (CK_A' - C_{ads})$$

and the mass balance in the gas phase is:

$$V \frac{\partial C}{\partial z} + \frac{\partial C}{\partial t} + \rho_p \frac{1-\epsilon}{\alpha} \frac{\partial C_{ads}}{\partial t} = 0$$

Derivation of the moments equations for the above model yields:

$$M_0 = z/V \frac{1-\epsilon}{\alpha} \rho_p K_A' = W_t/Q K_A$$

$$(M_1/M_0^2 - 1/2) W_t/Q = \frac{1}{UA}$$

The differential equations were solved using the procedure outlined by Pigford and Marshall⁵ and were also put into the form presented by Masamune and Smith² for comparison. (See Table 2.) For the cases of k_f controlling or k_{ads} controlling (i.e., making the substitutions $UA = k_f A$ or $UA = k_{ads} \delta$, respectively), the overall coefficient model is identical to the two corresponding single resistance models. For the case of pore diffusion controlling, the overall coefficient model gives the same results within the range of experimental error, i.e., it is impossible to differentiate between the two models. Comparisons of the overall coefficient model with the pore diffusion control-

⁵Marshall, W. R., Jr., and R. L. Pigford, "The Application of Differential Equations to Chemical Engineering Problems", University of Delaware, Newark, Delaware (1947).

ling model are listed in Tables 3 - 5. These results show that C/C_0 differs less than 0.012 for all points, and for most points the difference is much less. The largest difference in the two models occurs at breakthrough; however, this difference is not significant since the experimentally determined values of C/C_0 at breakthrough are very difficult to obtain accurately due to the very low concentrations exiting the bed. For example, with a reference peak height of two inches, a C/C_0 value of 0.01 would require measuring very accurately a peak height of 0.02 inches. The range of UA and K_A shown in Tables 3 - 5 represent extremes not found in this study but are presented here to illustrate the similarity between models. The comparison for $UA = 5.9850 - 7.9785$ with $K_A = 15.53$ is representative of bolt 3 foam material, whereas the comparison of models for $UA = 3.9900 - 5.9850$ with $K_A = 7.76 - 11.64$ best represents bolt 2 foam material.

RESULTS

Some of the modeling results are shown in Figures 2 - 6 for bolt 3 carbon impregnated foam material. The model prediction is shown as a solid line and the experimental data are plotted as symbols. Figures 2 and 3 present data from typical one and three layer runs on a conditioned sample of bolt three material and show excellent agreement of model and experimental results. Figures 4, 5, and 6 show experimental data and model prediction for three types of conditions, and except for the somewhat scattered data in Figure 6, the agreement is excellent. These results indicate that the model is adequate for predicting breakthrough curves in cases when the foam material's adsorptive capacity may have been altered by sweat poisoning, addition of water, or removal of water. The run conditions of Figure 6 represent the upper range of flow rate and concentration used in this investigation, and the experimental scatter is probably due to the very rapid rise of the breakthrough curve with limited sampling time. Since K_A and the rate parameter UA are calculated from the experimental data, the poor fit by the model in Figure 6 must be due to inaccurate data. The model is helpful even with scattered data as it fits a smooth continuous curve through the experimental points.

Figure 7 shows the effect of changing the equilibrium adsorption constant, K_A , as predicted by the model. The characteristic shape of the curve is the same but the area is different. This reflects a change in the total amount adsorbed which is proportional to the area under the $1 - C/C_0$ curve and proportional to K_A .

Figure 8 shows the effect of changing the overall coefficient by $\pm 25\%$. The curve for $UA = 7.9785$ goes between the two shown and is left out to show more effectively the change in the curve's characteristic shape. The transmission curve is not very sensitive to changes in UA and indicates that small variations in the rate parameter due to experimental error may be acceptable. The area under the $1 - C/C_0$ curve is the same for both curves drawn and reflects the fact that K_A (and thus total amount adsorbed) was held constant.

The three independent variables that influence carbon tetrachloride adsorption are temperature (T), concentration of the carbon tetrachloride in the inlet gas stream (C_0) and flow rate through the sample (Q). A central composite statistical design of experiments was set up to determine quantitatively the effects of these variables on the equilibrium constant, K_A , and on the overall mass transfer coefficient, UA . A linear fit of K_A with the three run variables showed the equilibrium constant to be a significant function of concentration and temperature given below for bolt 2 carbon impregnated foam material:

$$K_A = 17.4 - 0.58 C_0 - 0.12 T$$

for $5.2 \text{ mg/l} \leq C \leq 12.5 \text{ mg/l}$

$$25^\circ\text{C} \leq T \leq 40^\circ\text{C}$$

with a standard deviation of 0.72 and a value of \bar{K}_A (mean) = 9.09.

As expected, the variation with flow rate, Q , was not statistically significant. These values of K_A from the dynamic adsorption runs (calculated from the zeroth moment equation) compared very favorably with the values obtained from the adsorption isotherms (from McBain balance). However, a

slight deviation was noticed at the higher concentrations where the isotherm has been found to be nonlinear. This is due to the assumption of a linear rate of removal made in the adsorption model, that is not valid for those concentrations in the nonlinear region of the adsorption isotherms.

A statistical fit for the overall coefficient for the statistical design experiments revealed that UA was a function of $1/C_0$ and Q:

$$UA = 2.10 + 4.80/C_0 + 0.75 Q$$

for $5.2 \text{ mg/l} \leq C_0 \leq 12.5 \text{ mg/l}$

$$0.5 \text{ l/min} \leq Q \leq 1.3 \text{ l/min}$$

with a standard deviation of 0.60 and a value of \overline{UA} (mean) = 3.060. The variation of UA with temperature, T, was not statistically significant; however, this was probably due to the small temperature range ($25^\circ\text{C} \leq T \leq 40^\circ\text{C}$) used.

Figure 9 shows the results of the above correlation produced from the statistical analysis of 38 runs, and the data points shown are average values of UA for specific run conditions. The figure shows clearly that UA is inversely proportional to inlet concentration and directly proportional to flow through the sample. This further indicates that the overall coefficient represents more than one resistance controlling since $D_c A/R$ should not be function of Q, flow through the sample, and $k_f A$ should not be a function of C_0 , inlet concentration.

The statistical analysis for bolt 2 foam material can be extended to predict the parameters UA and K_A for bolt 3 foam material. The functional dependence on run conditions is assumed to be the same for both bolts and the intercept used in the empirical correlations is determined from a randomly

picked run on bolt 3 material. Table 6 shows the result of breakthrough time comparisons for bolt 3 material based on the predicted values of the parameters, and except for one run at a low concentration, shows an excellent agreement of predicted and measured values for breakthrough time.

CONCLUSIONS

While the use of an overall coefficient model is not limited to complex adsorption systems, its chief advantage is the simple approach to modeling a system in which the controlling resistances are not known and are not easily found. The definition of an overall coefficient for an adsorption process is not exact in its description of the process, but it does provide a means of accounting for the effects of the three individual resistances in consistent units. This overall coefficient represents effectively a combined resistance, since each of the single resistance models fits the data equally well when the rate parameter is evaluated from the first moment equation.

The model works well for the carbon impregnated foam material for the range of flow, temperature, and inlet concentration used in this study. Extension of this model to systems using an adsorbent bed of cloth woven with carbon fibers, beds with inerts uniformly mixed in with an unknown quantity of adsorbent, and similar systems should be no problem. This model is especially advantageous for those systems in which flow through the bed is difficult to characterize, the amount of adsorbent in the bed is unknown, and in which various physical properties (such as α , ϵ , ρ_p , R) cannot be confidently and accurately determined. The elimination of the need for moments higher than the first moment is another advantage in treating data that is too inaccurate for higher (or complete) moment analysis. By setting up a simple statistical design of experiments, one can determine the overall coefficient, UA , as a function of the various run conditions and with this information the dynamics of adsorption can be characterized mathematically.

REFERENCES

1. Schneider, P., and J. M. Smith, AICHE J., 14, 762 (1968).
2. Masamune, S., and J. M. Smith, AICHE J., 11, 34 (1965).
3. Rosen, J. B., J. Chem. Phys., 20, 387 (1952).
4. Aris, R., Proc. Roy. Soc. (London), A245, 268 (1958).
5. Marshall, W. R., Jr., and R. L. Pigford, "The Application of Differential Equations to Chemical Engineering Problems", University of Delaware, Newark, Delaware (1947).

List of Symbols

A	surface area of active carbon particles per unit weight of foam material, cm^2/g
A_f	flow area of foam sample, cm^2
C	concentration of adsorbable gas in the interparticle space, mg/l
C_{ads}	concentration of adsorbed gas per unit weight of adsorbent, $\text{mg CCl}_4/\text{g particle}$
C_i	concentration of adsorbable gas in the intraparticle space, mg/l
C_0	initial concentration of CCl_4 , mg/l
D_c	effective interparticle diffusion coefficient, cm^2/sec
k_{ads}	adsorption rate constant, $\text{g particles}/(\text{mgCCl}_4 - \text{min})$
K_A	adsorption equilibrium constant, $\text{ml}/\text{g foam material}$
K_A'	adsorption equilibrium constant of pure carbon particles, ml/g
k_f	mass transfer coefficient, cm/sec
L	number of layers of foam material in the bed
M_0	zereth moment of t vs. $(1 - C/C_0)$ curve, min .
M_1	first moment, min^2
M_2	second moment, min^3
M_3	third moment, min^4
Q	flow through sample, l/min
R	radius of spherical particle of adsorbent, cm
r	length coordinate in the spherical particle of adsorbent, measured from the center of the particle, cm
T	temperature of sample and gas, $^\circ\text{C}$
t	time, min .
$1/UA$	overall mass transfer coefficient, $\text{ccCCl}_4/(\text{g foam-min})$
V	interstitial velocity, cm/min .
W_t	sample weight, g
z	length coordinate of bed of adsorbent, cm

Greek Letters

α	cloth porosity (void volume/total volume)
β	intraparticle void fraction of carbon particle
δ	weight of particles per unit weight of foam material

- ϵ void fraction representing the bed volume not occupied by carbon particles divided by the total volume
- ρ_m apparent density of foam material, g solids/cc total volume
- ρ_p apparent particle density, g carbon/cc carbon

TABLES

Table 1. Components of Experimental Apparatus (Figure 1)

1. Control Valve size $c_v = 0.038$
2. Control Valve size $c_v = 0.00145$
3. U-tube Manometer
4. Carbon Tetrachloride Bubbler Chilled at 0°C
5. Orifice Meter
6. Hook Gage Manometer
7. Control Valve size $c_v = 0.15$
8. Rotameter
9. Rotameter
10. On-off Valve
11. Rotameter
12. On-off Valve
13. Thermocouple
14. Temperature Equilibrating Coil
15. Tangential Entry of gas into Manifold to Facilitate Mixing
16. Wire Mesh Obstruction to Improve Mixing
17. Stainless Steel Manifold
18. On-off Valve
19. Sample Holder
20. U-tube Manometer
21. Thermocouple
22. Rotameter
23. Control Valve Size $c_v = 0.15$
24. Control Valve Size $c_v = 0.15$
25. Plexiglas Compartment
26. Exit for Reference Sampling

Table 2. Comparison of Models

controlling resistance:	$\underline{D_c}$ (pore diffusion)	$\underline{k_f}$ (mass transfer)	$\underline{k_{ads}}$ (adsorption)	\underline{UA} (overall coefficient)
mass balance in sphere	$D_c \left(\frac{\partial^2 C_i}{\partial r^2} + \frac{2}{r} \frac{\partial C_i}{\partial r} \right) - \frac{\partial C_i}{\partial t}$ $- \rho_p \frac{\partial C_{ads}}{\partial t} = 0$	$\frac{\partial C_i}{\partial r} = 0$	$\frac{\partial C_i}{\partial r} = 0$	$\frac{\partial C_i}{\partial r} = 0$
rate of removal, R	$\frac{D_c}{R} \frac{1-\epsilon}{\alpha} \left(\frac{\partial C_i}{\partial r} \right)_{r=R}$	$3/R \frac{1-\epsilon}{\alpha} k_f (C_i - \frac{C_{ads}}{K_A})$	$\frac{1-\epsilon}{\alpha} \rho_p k_{ads} \left(C_i - \frac{C_{ads}}{K_A} \right)$	$\frac{\partial C_{ads}}{\partial t} = \frac{UA}{\delta K_A} (CK_A - C_{ads})$
mass balance in gas phase	$-V \frac{\partial C}{\partial z} - \frac{\partial C}{\partial t} - R = 0$	same	same	same
solution	$C/C_0 = \frac{1}{2} + \frac{2}{\pi} \int_0^{\alpha_1} e^{-\lambda^2 t} \sin \frac{\alpha_2 \lambda}{\lambda}$	same	same	same
	$\alpha_1 = \frac{W_t}{Q} (D_c A/R) \phi_1$	$\alpha_1 = \frac{W_t}{Q} (k_f A) \phi_1$	$\alpha_1 = \frac{W_t}{Q} (k_{ads} V) \phi_1$	$\alpha_1 = \frac{W_t}{Q} UA \phi_1$

Table 2 (continued)

$$\alpha_2 = \frac{2}{3K_A} (D_c A/R) \lambda^2 \tau - \frac{M_t}{Q} (D_c A/R) \phi_2$$

$$\alpha_2 = \frac{(k_f A)}{K_A} \lambda^2 \tau$$

$$\alpha_2 = \frac{(k_{ads} \delta)}{K_A} \lambda^2 \tau$$

$$\alpha_2 = \frac{UA}{K_A} \lambda^2 \tau$$

$$\phi_1 = \frac{\lambda (\sinh 2\lambda + \sin 2\lambda)}{\cosh 2\lambda - \cos 2\lambda} - 1$$

$$\phi_1 = \lambda^4 / 1 + \lambda^4$$

$$\phi_1 = \lambda^4 / 1 + \lambda^4$$

$$\phi_1 = \lambda^4 / 1 + \lambda^4$$

$$\phi_2 = \frac{\lambda (\sin 2\lambda - \sinh 2\lambda)}{\cosh 2\lambda - \cos 2\lambda}$$

$$\phi_2 = \lambda^2 / 1 + \lambda^4$$

$$\phi_2 = \lambda^2 / 1 + \lambda^4$$

$$\phi_2 = \lambda^2 / 1 + \lambda^4$$

$$-\frac{M_t}{Q} (k_f A) \phi_2$$

$$-\frac{M_t}{Q} (k_{ads} \delta) \phi_2$$

$$-\frac{M_t}{Q} UA \phi_2$$

Table 3. Comparison of Model Results - Varying UA

Model 1 - $D_c A/R$ controlling model

Model 2 - $k_f A, k_{ads} \delta$, or UA model

$$K_A = 15.53$$

$$UA = 3.9900$$

$$UA = 5.9850$$

$$UA = 7.9785$$

$$UA = 9.9735$$

Time (min)	Model 1 $\frac{C}{C_0}$	Model 2 $\frac{C}{C_0}$	Model 1 $\frac{C}{C_0}$	Model 2 $\frac{C}{C_0}$	Time (min)	Model 1 $\frac{C}{C_0}$	Model 2 $\frac{C}{C_0}$	Model 1 $\frac{C}{C_0}$	Model 2 $\frac{C}{C_0}$
30	0.000	0.000	0.000	0.000	40	0.000	0.000	0.000	0.000
40	0.028	0.39	0.008	0.014	50	0.029	0.035	0.016	0.021
50	0.102	0.109	0.054	0.061	60	0.128	0.131	0.199	0.102
75	0.474	0.464	0.449	0.443	70	0.316	0.316	0.290	0.292
100	0.808	0.807	0.846	0.845	100	0.876	0.876	0.899	0.900
125	0.952	0.955	0.977	0.980	125	0.989	0.991	0.994	0.996

Table 4. Comparison of Model Results - Varying K_A
 Model 1 - $D_{cA/R}$ controlling model
 Model 2 - $k_f A$, k_{ads} , or UA model

UA = 7.9785
 $K_A = 3.88$

$K_A = 11.64$

$K_A = 19.41$

Time (min)	Model 1 $\frac{(C/C_0)}{}$	Model 2 $\frac{(C/C_0)}{}$	Time (min)	Model 1 $\frac{(C/C_0)}{}$	Model 2 $\frac{(C/C_0)}{}$	Time (min)	Model 1 $\frac{(C/C_0)}{}$	Model 2 $\frac{(C/C_0)}{}$
10	0.000	0.000	25	0.000	0.000	50	0.000	0.000
15	0.128	0.131	30	0.000	0.000	60	0.020	0.026
20	0.545	0.536	40	0.052	0.058	65	0.042	0.048
25	0.876	0.877	50	0.246	0.242	75	0.128	0.131
30	0.980	0.983	75	0.876	0.877	100	0.545	0.535
40	1.000	1.000	100	0.996	0.997	125	0.876	0.876

Table 5. Comparison of Model Results - Varying k_A and UA

Model 1 - $D_c A/R$ controlling model

Model 2 - $k_f A$, k_{ads} , or UA model

$$k_A = 3.88$$

$$UA = 1.9950$$

$$k_A = 7.76$$

$$UA = 3.9900$$

$$k_A = 11.64$$

$$UA = 5.9850$$

$$k_A = 19.41$$

$$UA = 9.9735$$

Time (min)	Model 1 $\frac{C/C_0}{(C/C_0)}$	Model 2 $\frac{C/C_0}{(C/C_0)}$	Model 1 $\frac{C/C_0}{(C/C_0)}$	Model 2 $\frac{C/C_0}{(C/C_0)}$	Model 1 $\frac{C/C_0}{(C/C_0)}$	Model 2 $\frac{C/C_0}{(C/C_0)}$	Time (min)	Model 1 $\frac{C/C_0}{(C/C_0)}$	Model 2 $\frac{C/C_0}{(C/C_0)}$
5	0.004	0.018	0.000	0.000	0.000	0.000	40	0.000	0.000
15	0.331	0.319	0.003	0.009	0.000	0.000	50	0.001	0.002
25	0.755	0.745	0.102	0.109	0.001	0.003	55	0.003	0.006
30	0.873	0.872	0.229	0.226	0.008	0.014	60	0.010	0.014
40	0.972	0.977	0.554	0.541	0.083	0.090	65	0.025	0.030
50	0.995	0.997	0.808	0.804	0.284	0.278	70	0.053	0.059
75	1.000	1.000	0.991	0.993	0.847	0.846	75	0.099	0.102
100	1.000	1.000	1.000	1.000	0.989	0.991	100	0.543	0.535
125	1.000	1.000	1.000	1.000	1.000	1.000	125	0.899	0.900

Table 6. Model Prediction of Breakthrough Time for Bolt 3 Foam Material.

Run No.	C_0	Q	T	$UA/15(\text{meas.})$	$UA/15(\text{pred.})$	$K_A(\text{meas.})$	$K_A(\text{pred.})$	$t_b^*(\text{meas.})$	$t_b^*(\text{pred.})$
3-1	10.45	1.3	37	1.3827	0.5419	12.13	13.36	122	122
3-2	5.24	0.7	37	0.4190	0.5425	19.21	16.38	95.5	87
3-3	10.30	1.3	37	0.5735	0.5423	12.54	13.46	29	30.05
3-4	10.45	1.0	40	0.4953	0.5269	12.58	13.00	41	42
3-5	3.15	1.0	32	1.0213	0.5978	29.38	18.19	399	238
3-17**	7.86	1.0	32.5	0.5373	0.5469	15.41	15.41	185	183
3-23	10.45	1.3	37	0.6186	0.5419	12.36	13.36	33.5	32
3-13	7.86	1.3	32.5	0.5319	0.5369	15.53	15.41	54	53

*time at which $C/C_0 = 0.05$

**Used as basis for determining the intercepts in the following equations:

$$K_A(\text{pred.}) = 23.86 - .58C_0 - .12T, \quad UA(\text{pred.}) = .4463 + .32/C_0 + .05Q$$

FIGURES

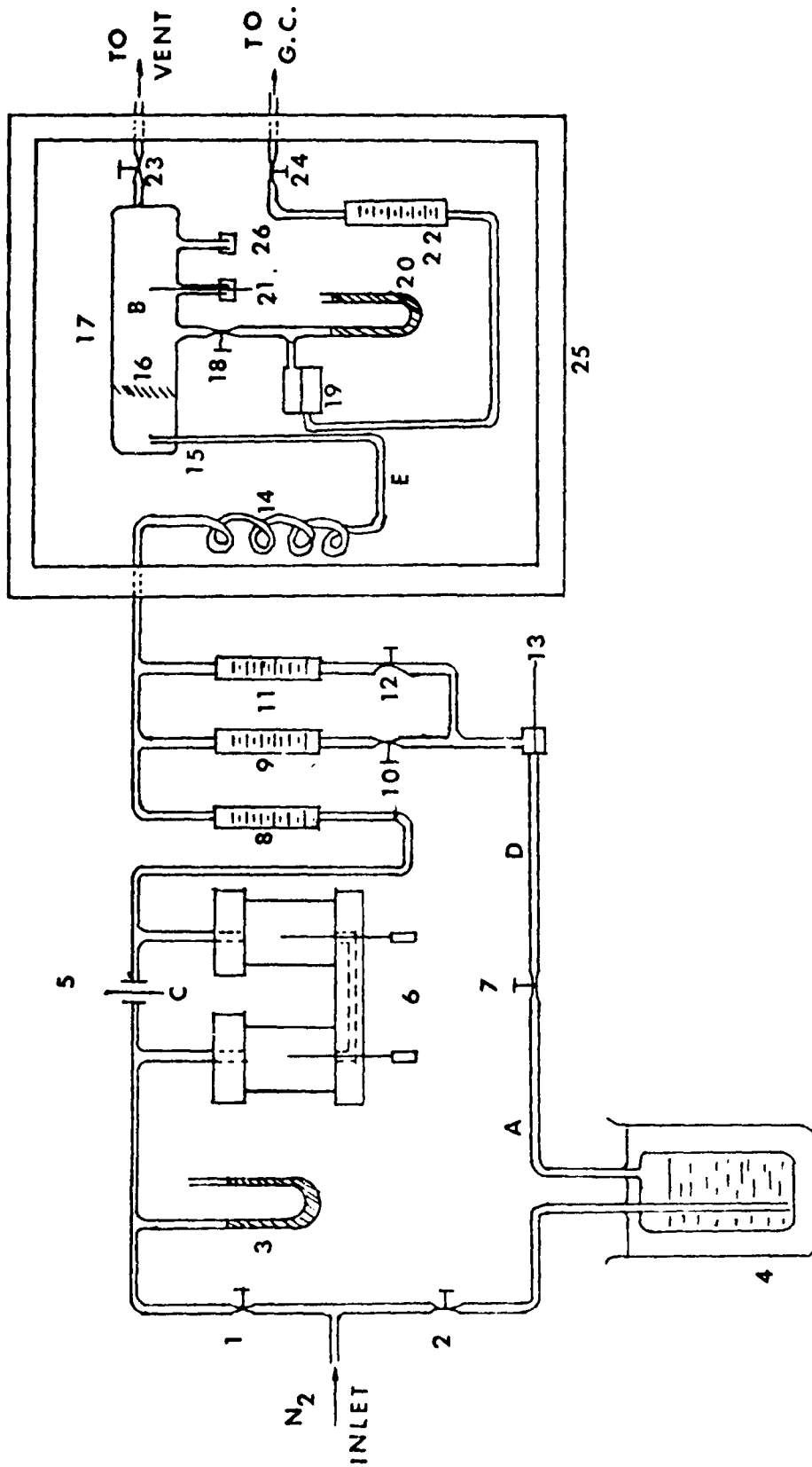


Figure 1. Schematic of Vapor Test Apparatus.

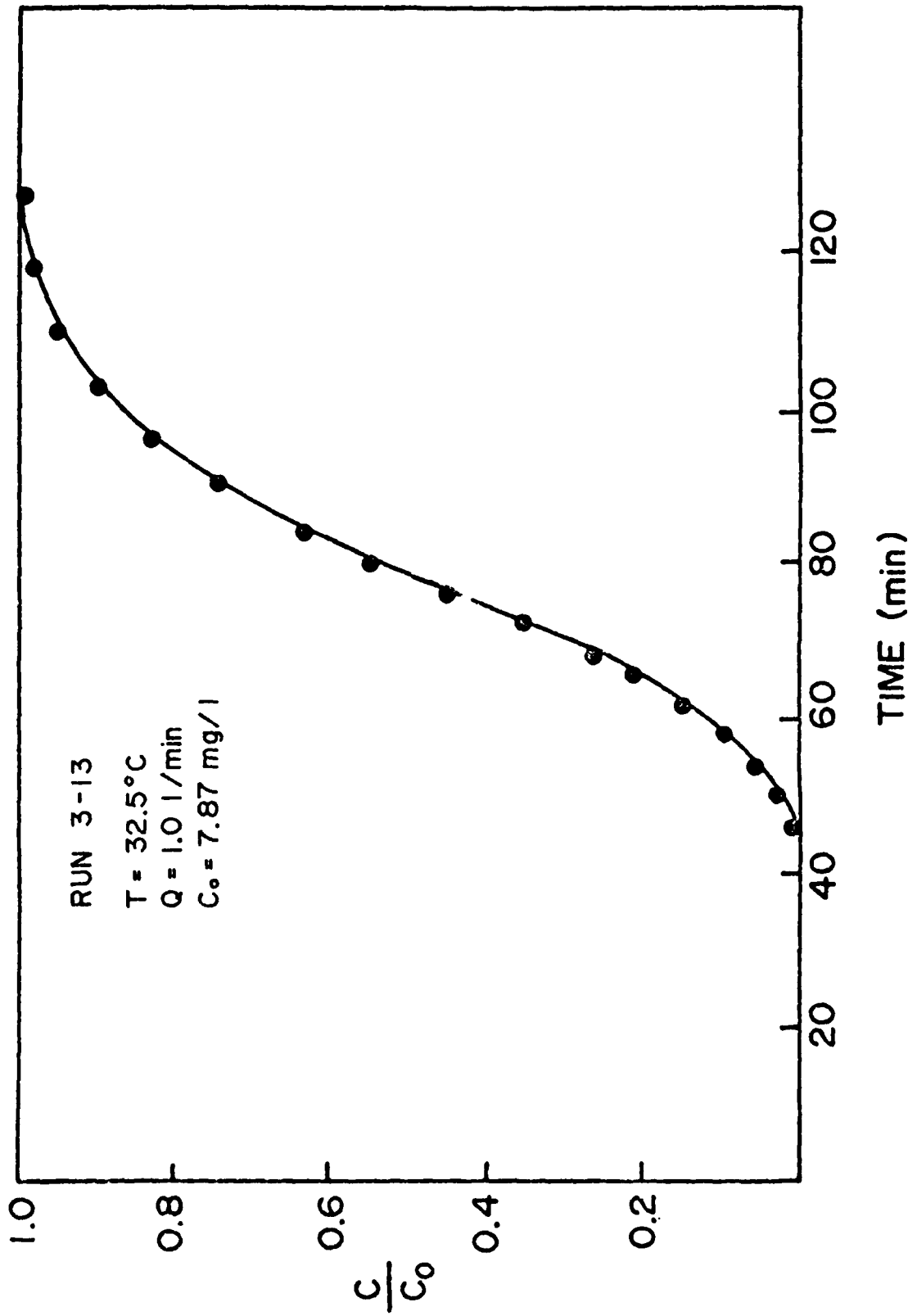


Figure 2. Model Prediction and Experimental Data for One Layer Run.

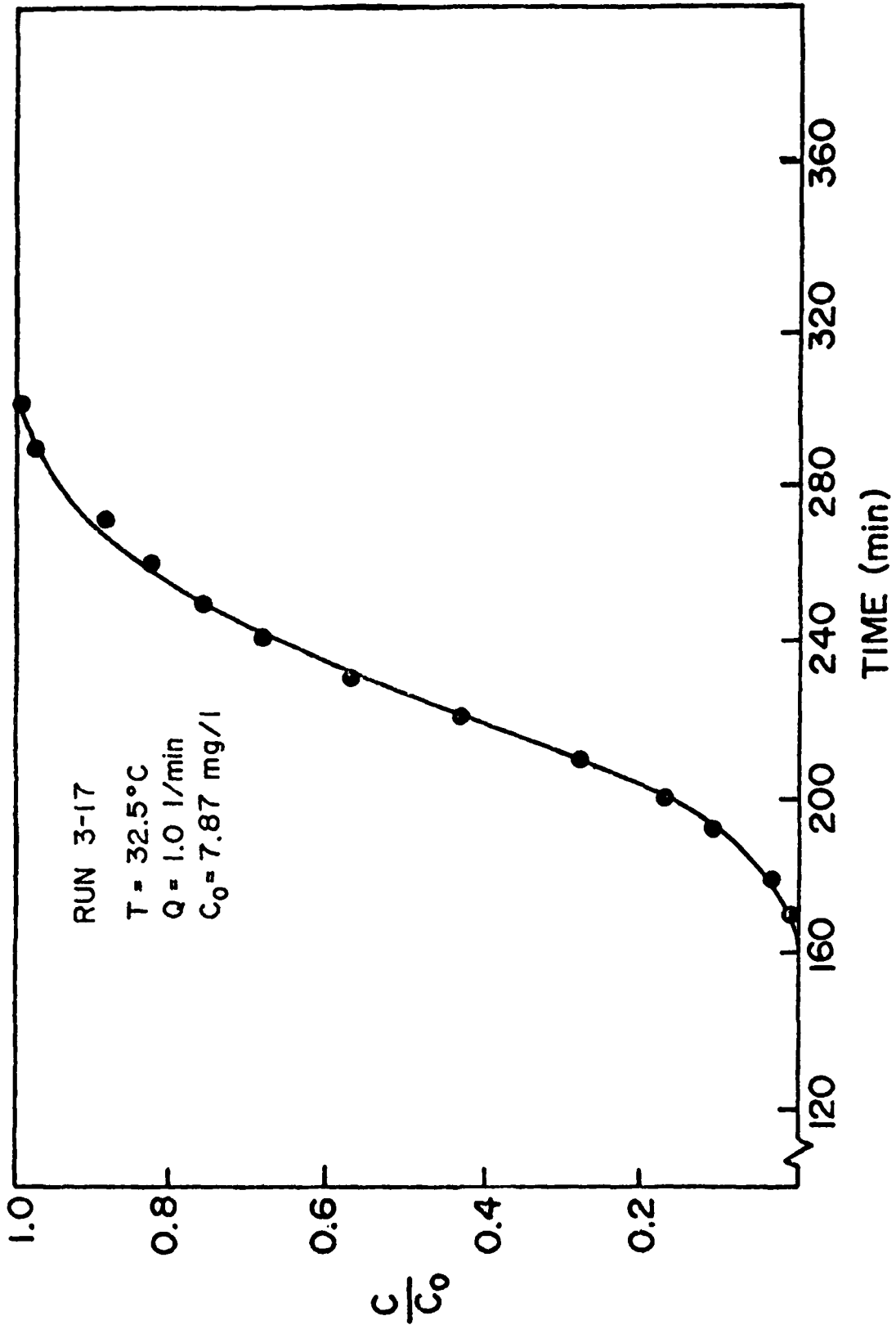


Figure 3. Model Prediction and Experimental Data for Three Layer Run.

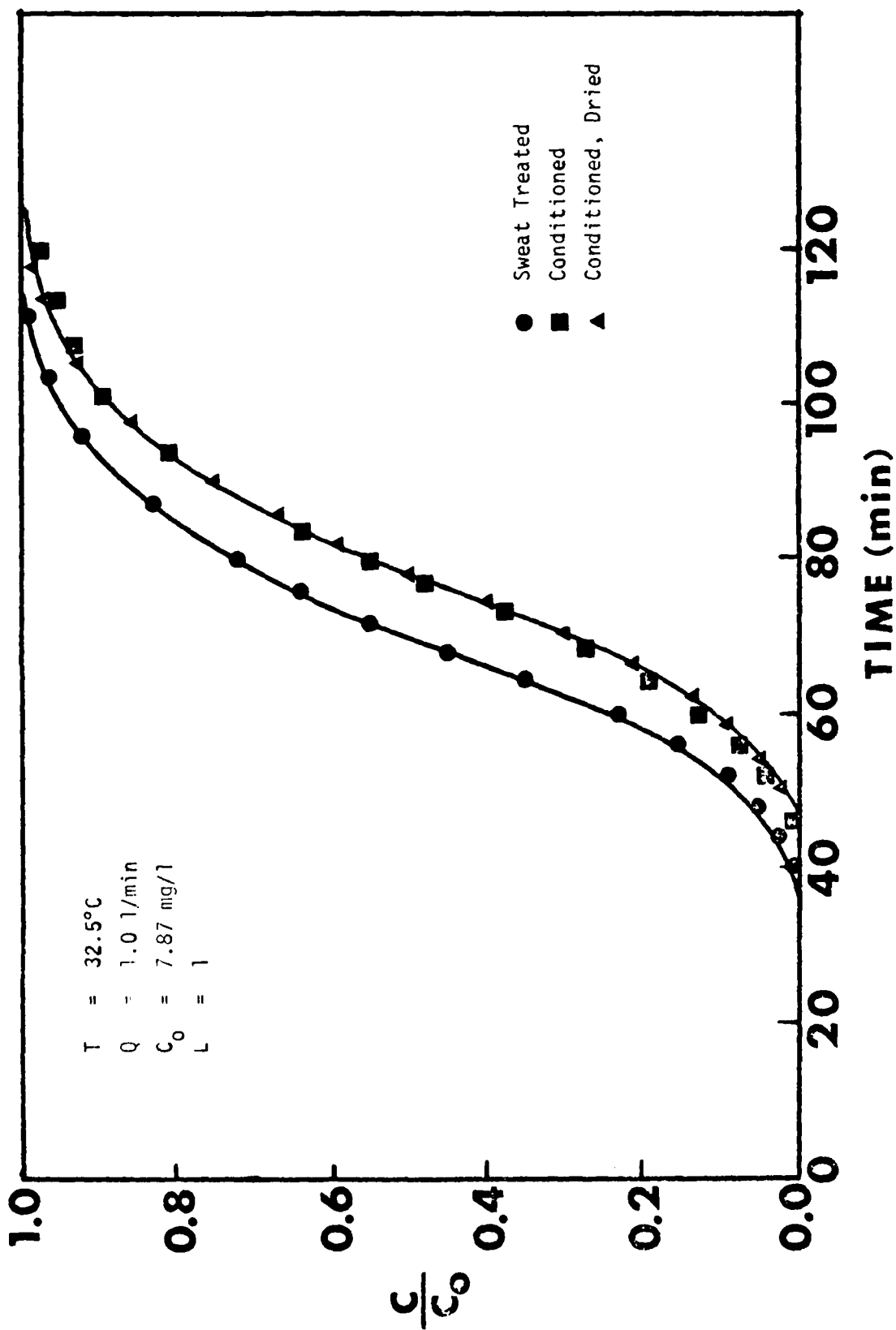


Figure 4. Model and Experimental Data for Different Conditions.

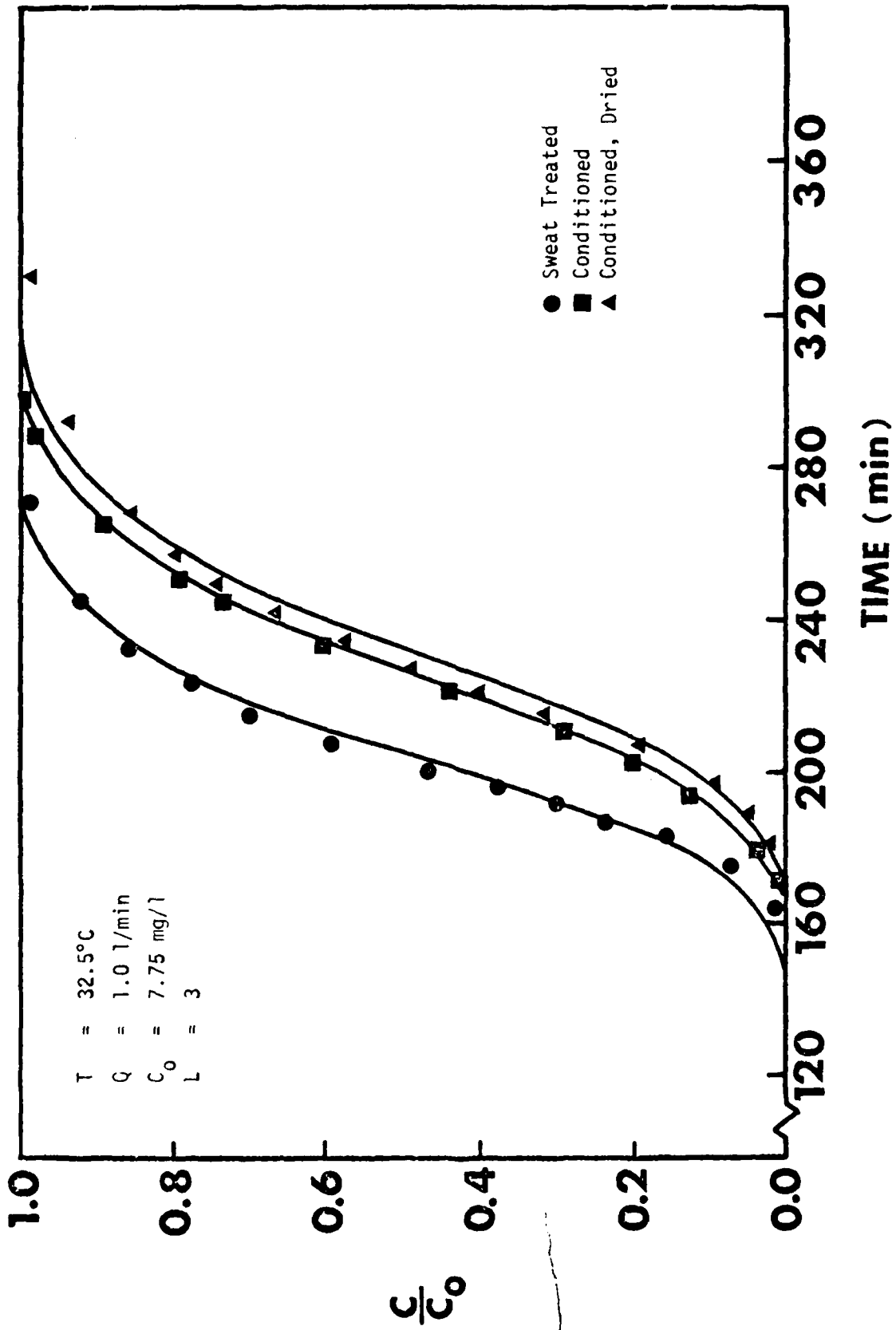


Figure 5. Model and Experimental Data for Different Conditions.

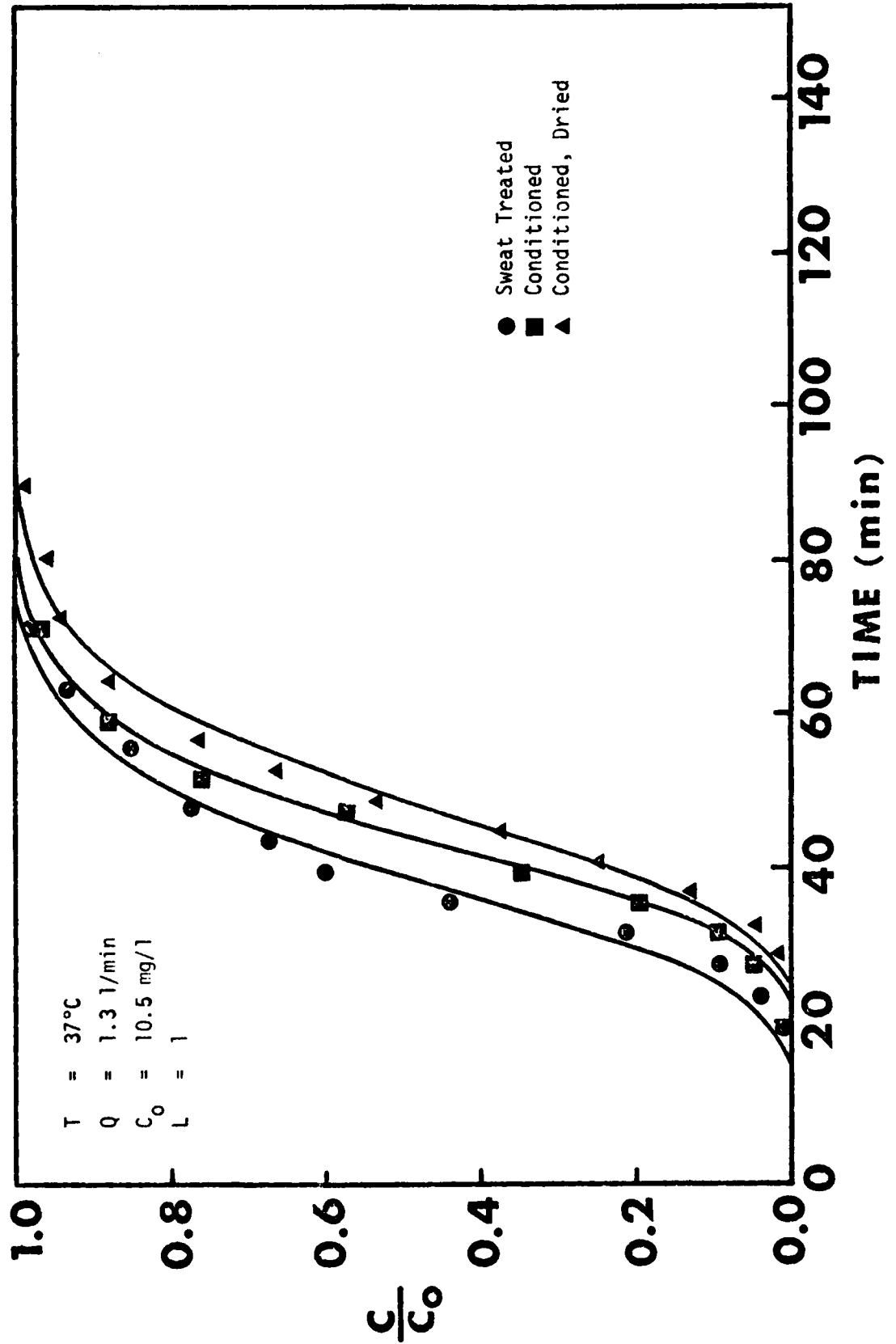


Figure 6. Model and Experimental Data for Different Conditions.

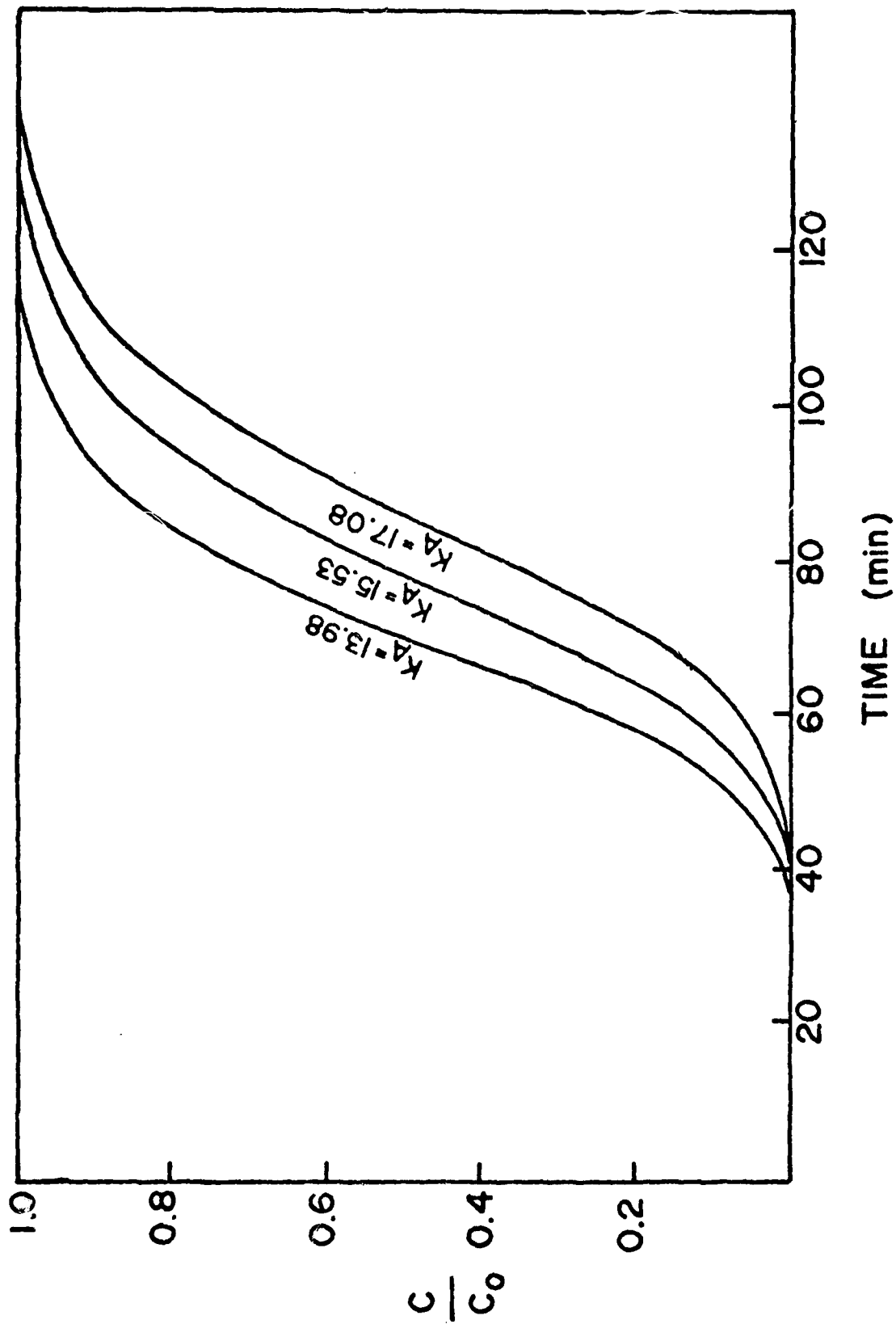


Figure 7. Effect of Changing K_A 10 % as Predicted by Mathematical Model.

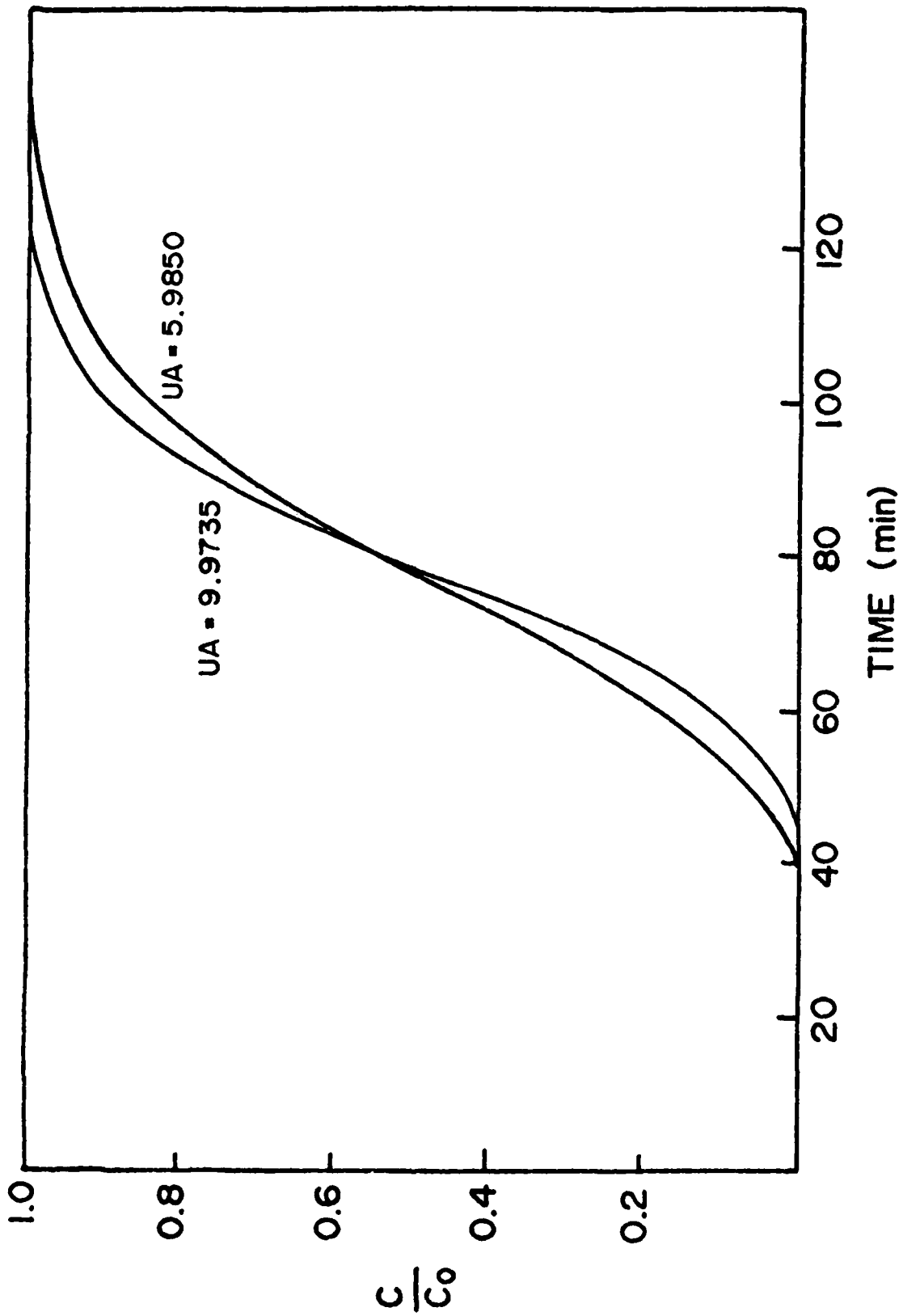


Figure 8. Effect of Changing UA 25 % as Predicted by Mathematical Model.

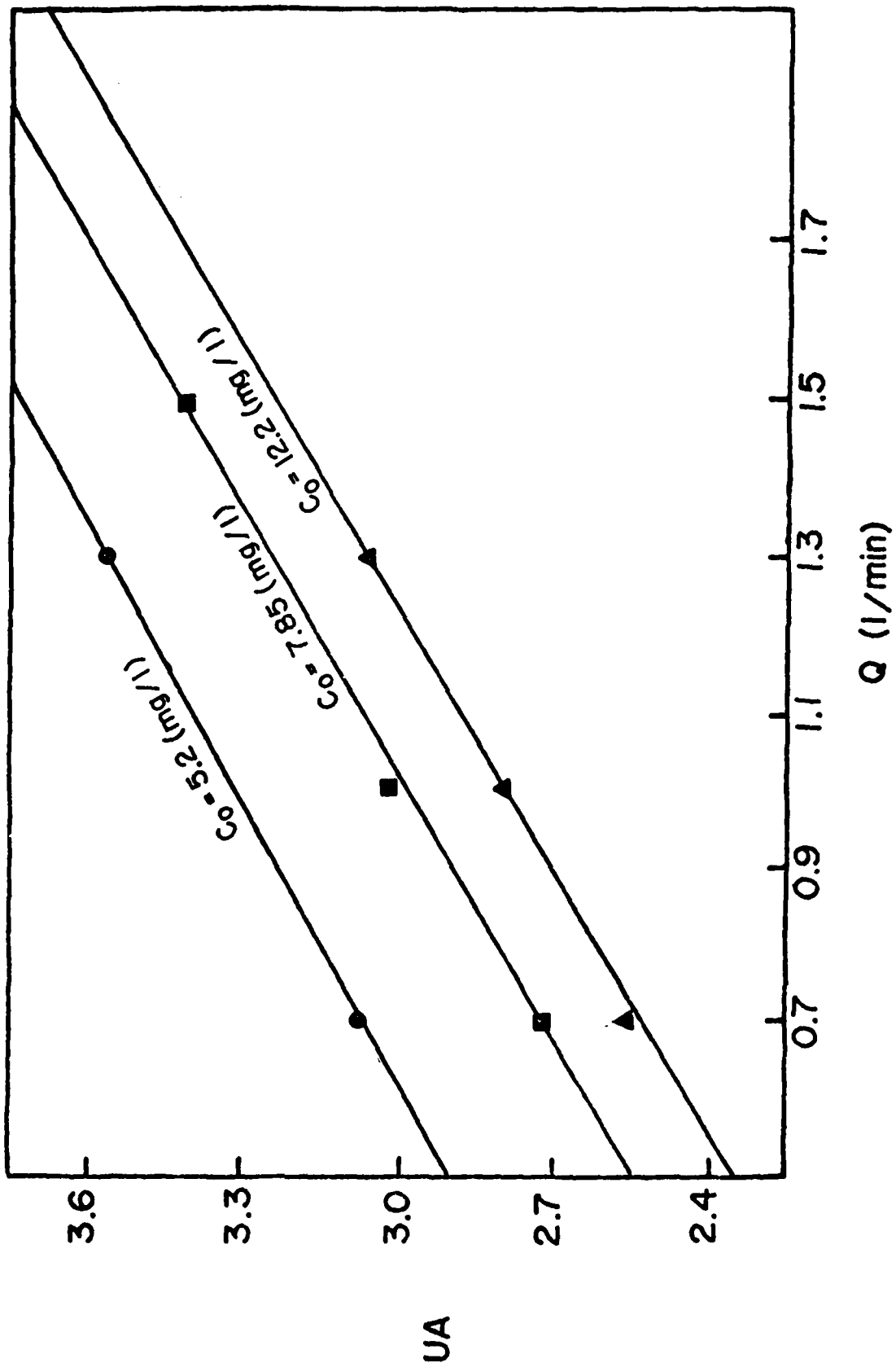


Figure 9. Correlation of UA from Statistical Analysis.

Derivation of Zeroth and First Moment Equations

mass balance of the adsorbable component in the gas phase:

$$-v \frac{\partial C}{\partial z} - \frac{\partial C}{\partial t} - \frac{3D_c}{R} \frac{1-t}{\alpha} \left(\frac{\partial C_i}{\partial r} \right)_{r=R} = 0 \quad (1)$$

mass balance of this component in the particle:

$$\frac{D_c}{\beta} \left(\frac{\partial^2 C_i}{\partial r^2} + \frac{2}{r} \frac{\partial C_i}{\partial r} \right) - \frac{\partial C_i}{\partial t} - \frac{\rho_p}{\beta} \frac{\partial C_{ads}}{\partial t} = 0 \quad (2)$$

rate of adsorption (assumed to be linear):

$$\frac{\partial C_{ads}}{\partial t} = k_{ads} (C_i - C_{ads}/K_A') \quad (3)$$

external diffusion boundary condition:

$$D_c \left(\frac{\partial C_i}{\partial r} \right)_{r=R} = k_f (C - C_i) \quad (4)$$

internal diffusion boundary condition:

$$\frac{\partial C_i}{\partial r} = 0 \quad \text{at } r = 0 \quad \text{for } t > 0 \quad (5)$$

and the initial conditions

$$C = 0 \quad \text{at } z > 0 \quad \text{for } t = 0 \quad (6)$$

$$C_i = 0 \quad \text{at } r \geq 0 \quad \text{for } t = 0 \quad (7)$$

$$C = C_0 \quad \text{at } z = 0 \quad \text{for } t > 0 \quad (8)$$

Derivation of Laplace transforms of mass balance equations

$$L[C_i(z,r,t)] = \bar{C}_i(z,r,s)$$

$$\text{Eq. (2)} \rightarrow \frac{D_c}{\beta} \left(\frac{d^2 \bar{C}_i}{dr^2} + \frac{2}{r} \frac{d\bar{C}_i}{dr} \right) - s\bar{C}_i - s \frac{\rho_p}{\beta} \bar{C}_{ads} = 0 \quad (9)$$

$$\text{Eq. (3)} \rightarrow S\bar{C}_{\text{ads}} = k_{\text{ads}}\bar{C}_i - \frac{k_{\text{ads}}}{K_A'}\bar{C}_{\text{ads}} \rightarrow \bar{C}_{\text{ads}} = \left(\frac{k_{\text{ads}}}{S+k_{\text{ads}}\frac{K_A'}{K_A'}}\right)\bar{C}_i \quad (10)$$

substitute (10) into (9) \rightarrow

$$\frac{d^2\bar{C}_i}{dr^2} + \frac{2}{r}\frac{d\bar{C}_i}{dr} - \frac{S\beta\bar{C}_i}{D_c} - \frac{S\rho_p}{D_c}\left(\frac{k_{\text{ads}}}{S+k_{\text{ads}}\frac{K_A'}{K_A'}}\right)\bar{C}_i = 0 \quad (11)$$

$$= \frac{d^2\bar{C}_i}{dr^2} + \frac{2}{r} + \lambda\bar{C}_i = 0 \quad (12)$$

$$\text{where } \lambda = \frac{S}{D_c}\left[\beta + \frac{\rho_p k_{\text{ads}}}{S+k_{\text{ads}}\frac{K_A'}{K_A'}}\right] \quad (13)$$

Transforming boundary conditions:

$$\frac{\partial\bar{C}_i}{\partial r}(z,0,t) = 0 \rightarrow \frac{d\bar{C}_i}{dr}(Z,0,S) = 0 \quad (14)$$

$$\frac{\partial\bar{C}_i}{\partial r}(z,R,S) = \frac{k_f}{D_c}[\bar{C}(S,z) - \bar{C}_i(S,R)] \quad (15)$$

Solution of (12) is:

$$\bar{C}_i(z,r,S) = E/r \sin r\sqrt{\lambda} \quad (16)$$

$$\rightarrow \frac{d\bar{C}_i}{dr}(z,R,S) = E\left[-\frac{\sqrt{\lambda}}{R}\cos R\sqrt{\lambda} - \frac{1}{R^2}\sin R\sqrt{\lambda}\right] \quad (17)$$

Equating (15) and (17) \rightarrow

$$E = \frac{k_f}{D_c}\bar{C}(S,z)/\left[-\frac{\sqrt{\lambda}}{R}\cos R\sqrt{\lambda} - \frac{1}{R^2}\sin R\sqrt{\lambda}\right] + \frac{k_f}{D_c R}\sin R\sqrt{\lambda} \quad (18)$$

Now take the Lapalce transform of Eq. (1)

$$-v \frac{d\bar{C}}{dz} - S\bar{C} - \frac{3D_c}{R} \frac{1-\epsilon}{\alpha} \left(\frac{d\bar{C}_i}{dr} \right)_{r=R} = 0 \quad (19)$$

from (19) and (18)

$$\frac{d\bar{C}_i}{dr} (z, R, S) = \frac{(k_f/D_c)(\sqrt{\lambda}/R \cos R\sqrt{\lambda} - 1/R^2 \sin R\sqrt{\lambda})\bar{C}(S, z)}{\sqrt{\lambda}/R \cos R\sqrt{\lambda} - 1/R^2 \sin R\sqrt{\lambda} + k_f/D_c R \sin R\sqrt{\lambda}} \quad (20)$$

$$\rightarrow \frac{d\bar{C}_i}{dr} (z, R, S) = M\bar{C}(z, S) \quad (21)$$

$$\text{where } M = 1 - \frac{1}{D_c/k_f \sqrt{\lambda} \cot R\sqrt{\lambda} + (1 - D_c/k_f R)} \quad (22)$$

Let $1/L = \frac{3k_f}{VR} \frac{1-\epsilon}{\alpha}$ and substitute with (21) and (22) into (19)

$$-v \frac{d\bar{C}}{dz} - S\bar{C} - \frac{VM}{L} \bar{C} = 0 \quad (23)$$

$$\frac{d\bar{C}}{dz} + \left(\frac{S}{v} + \frac{M}{L} \right) \bar{C} = 0 \quad (24)$$

Transform boundary conditions;

$$\text{at } z = 0, c(0, t) = C_0 \rightarrow \bar{C}(0, S) = \frac{C_0}{S} \quad (25)$$

solution to (24) is

$$\bar{C}(z, S) = \frac{C_0}{S} e^{-S z/v - M/L z} = \frac{C_0}{S} e^{-S z/v} e^{-M/L z} \quad (26)$$

z/v = residence time in bed, assumed to be very small when compared with M/Lz so that (26) becomes

$$\bar{C}(z, S) = \frac{C_0}{S} e^{-M/L z} \quad (27)$$

$$\text{Define } G(z,t) = 1 - \frac{c(z,t)}{c_0} \quad (28)$$

$$\bar{G}(z,S) = \frac{1}{S} - \frac{\bar{c}(z,S)}{c_0} \quad (29)$$

Substituting (27) into (29) yields the transform $\bar{G}(z, S)$

$$\bar{G}(z,S) = \frac{1}{S} (1 - e^{-M/Lz}) \quad (30)$$

$$\text{where } M/L = \frac{3D_c}{VR} \frac{1-\epsilon}{\alpha} \left(1 - \frac{1}{\frac{D_c}{k_f} \sqrt{\lambda} \cot R \sqrt{\lambda} + (1 - \frac{D_c}{k_f R})} \right) \quad (31)$$

$$\text{and } \lambda = -\frac{S}{D_c} \left[\beta + \frac{\rho p_{ads}^k}{S + k_{ads}/K_A'} \right] \quad (32)$$

Derivation of the 0th moment of $\bar{G}(S, z)$

using Aris' theorem:

$$M_0 = \lim_{S \rightarrow 0} \bar{G}(z,S) = \lim_{S \rightarrow 0} 1/S [1 - e^{-M/Lz}] \rightarrow \frac{0}{0}$$

applying L'Hopital's' rule:

$$M_0 = \lim_{S \rightarrow 0} z \frac{d(M/L)}{dS} e^{-M/Lz} = \lim_{S \rightarrow 0} z \frac{d(M/L)}{dS}$$

$$\text{expand } \cot R \sqrt{\lambda}: \cot x = \frac{1}{x} - \frac{x}{3} - \frac{x^3}{45} \dots$$

$$\frac{d(M/L)}{dS} = \frac{3k_f}{RV} \frac{1-\epsilon}{\alpha} \frac{dG(\lambda)}{dS} \quad \text{where } G(\lambda) = 1 - \frac{1}{\frac{D_c}{k_f} \sqrt{\lambda} \cot R \sqrt{\lambda} + 1 - \frac{D_c}{k_f R}}$$

$$G(\lambda) \approx 1 - \frac{1}{\frac{D_c}{k_f} \sqrt{\lambda} \left[\frac{1}{R \sqrt{\lambda}} - \frac{R \sqrt{\lambda}}{3} \right] + 1 - \frac{D_c}{k_f R}}$$

$$\approx 1 - \frac{1}{1 - \frac{D_c R \lambda}{3k_f}}$$

$$\frac{dG(\lambda)}{dS} = \left(1 - \frac{D_c R \lambda}{3k_f}\right)^{-2} (-1) \frac{D_c R}{k_f^3} \frac{d\lambda}{dS}$$

$$\frac{d\lambda}{dS} = (-) \left[\frac{\beta}{D_c} + \left(\frac{\rho k_{ads}}{D_c} \frac{k_{ads}/K_A'}{(S + k_{ads}/K_A')^2} \right) \right]$$

$$M_0 = \lim_{S \rightarrow 0} \frac{z d(M/L)}{dS} = \lim_{S \rightarrow 0} \frac{3k_f}{RV} \frac{1-\epsilon}{\alpha} \left(\frac{D_c R \lambda}{k_f^3} + 1 \right)^{-2} \frac{D_c R}{3k_f} \left[\frac{\beta}{D_c} + \frac{\rho k_{ads}}{D_c} \frac{k_{ads}/K_A'}{(S + k_{ads}/K_A')^2} \right]$$

$$M_0 = \frac{z}{V} \frac{1-\epsilon}{\alpha} (\beta + \rho_p K_A') \quad (32)$$

Derivation of 1st moment

$$\begin{aligned} M_1 &= - \lim_{S \rightarrow 0} \frac{d\bar{G}(z, S)}{dS} = - \lim_{S \rightarrow 0} \frac{d(1/S(1 - e^{-M/Lz}))}{dS} \\ &= - \lim_{S \rightarrow 0} \frac{d(M/L)}{dS} \frac{ze^{-M/Lz} - (1)(1 - e^{-M/Lz})}{S^2} \rightarrow \frac{0}{0} \end{aligned}$$

applying L'Hopitals' rule twice:

$$M_1 = - \lim_{S \rightarrow 0} z \frac{d^2(M/L)}{dS^2} - \frac{M_0^2}{2}$$

must find $-\lim_{S \rightarrow 0} \frac{d^2(M/L)}{dS^2}$

$$G(\lambda) \approx 1 - \frac{1}{\frac{D_c}{k_f} \sqrt{\lambda} \left[\frac{1}{R \sqrt{\lambda}} = \frac{R \sqrt{\lambda}}{3} - \frac{R^3 (\sqrt{\lambda})^3}{45} \right] + 1 - \frac{D_c}{k_f R}}$$

$$G(\lambda) \approx 1 - \frac{1}{1 - \frac{D_c R \lambda}{3k_f} - \frac{R^3 D_c \lambda^2}{45k_f}}$$

$$\lim_{S \rightarrow 0} \frac{d^2 G(\lambda)}{dS^2} = \lim_{S \rightarrow 0} - \left(\frac{d\lambda}{dS} \right)^2 \left[\frac{2D_c R^3}{45k_f} - \frac{2D_c^2 R^2}{k_f^2 9} \right] - \frac{d^2 \lambda}{dS^2} \cdot \frac{D_c R}{k_f^3}$$

$$\frac{d^2 \lambda}{dS^2} = (-2) \frac{\rho_p k_{ads}}{D_c} \cdot \frac{k_{ads}}{K_A'} \left(S + \frac{k_{ads}}{K_A'} \right)^{-3}$$

$$\lim_{S \rightarrow 0} \frac{d^2 \lambda}{dS^2} = (-2) \rho_p K_A'^2 / D_c k_{ads}$$

$$\lim_{S \rightarrow 0} \frac{d^2(M/L)}{dS^2} = \frac{3k_f}{RV} \frac{1-\epsilon}{\alpha} \lim_{S \rightarrow 0} \frac{d^2 G(\lambda)}{dS^2}$$

$$\lim_{S \rightarrow 0} \left(\frac{d\lambda}{dS} \right)^2 = \left(\frac{\beta + \rho_p K_A'}{D_c} \right)^2$$

substituting the above three equations into the equation for M_1 yields:

$$M_1 = \left(\frac{z}{V} \frac{1-\epsilon}{\alpha} \right) \left[(\beta + \rho_p K_A')^2 \frac{R^2}{15D_c} + (\beta + \rho_p K_A')^2 \frac{R}{3k_f} + \frac{\rho_p K_A'^2}{k_{ads}} \right] + \frac{M_0^2}{2} \quad (33)$$

Explanation of Numerical Work

All integrals were evaluated numerically on a computer by using Simpson's rule. The integrals listed in Table (2) with an infinite upper limit were evaluated until the exponential damping factor, $\exp(-\alpha,)$, reached a value of 5×10^{-6} and a subsequent iteration increased the area by less than 5×10^{-4} percent. Pigford and Marshall (6) have solved the set of equations for the UA, k_{ads} , k_f model and have expressed it in the form of an integral with a finite upper limit. This solution, listed below, gave the same values for C/C_0 as the infinite integral expression listed in Table (2):

$$\frac{C(n, \tau)}{C_0} = 1 - e^{-\tau} \int_0^n e^{-\tau} I_0(2(n\tau)^{1/2}) d\tau$$

where $n = \frac{h j K_A' z}{V}$, $\tau = t h$, $j = \alpha_p \frac{1-\epsilon}{\alpha}$, $h = \frac{UA}{\delta K_A'}$